Rhizoma Paridis saponins ameliorates hepatic fibrosis in rats by downregulating expression of angiogenesis-associated growth factors

YANQUAN HAN[1], LINGYU PAN[1], SHAN RAN[2], YAN SONG[2], FANG-FANG SUN[2], YONG-ZHONG WANG[1] and YAN HONG[2]

[1]Grade 3 Laboratory of Traditional Chinese Medicine Preparation, The First Affiliated Hospital, Anhui University of Chinese Medicine, State Administration of Anhui University of Chinese Medicine; [2]School of Pharmacy, Anhui University of Chinese Medicine, Hefei, Anhui 230031, P.R. China

Received March 22, 2018; Accepted December 18, 2018

DOI: 10.3892/mmr.2019.10006

Abstract. Previously, we demonstrated that *Rhizoma Paridis* saponins (RPS), the major active component of *Rhizoma Paridis*, may exhibit hepatoprotective effects. The present study aimed to identify the potential mechanism of RPS on hepatic injury and improvement in hepatic fibrosis (HF). A HF model was created in Sprague-Dawley rats by administration of carbon tetrachloride. RPS was administered for treatment following creation of the HF model. The protein and mRNA expression of vascular endothelial growth factor (VEGF), platelet-derived growth factor (PDGF), extracellular signal-regulated kinase (ERK)1/2 and α-smooth muscle actin (SMA) was detected by reverse transcription quantitative polymerase chain reaction and western blot analysis. RPS was demonstrated to improve hepatic inflammation and decrease HF severity according to hematoxylin and eosin and Masson trichrome staining. Following RPS treatment, the level of alanine aminotransferase, aspartate aminotransferase and malondialdehyde, and expression levels of the mRNA and protein of VEGF, ERK1/2, PDGF and α-SMA in the model group was decreased. By contrast, the content of glutathione-PX and superoxide dismutase was increased. These data suggest that RPS may treat HF primarily through downregulation of the expression levels of the mRNA and phosphorylated VEGF, ERK1/2, PDGF and α-SMA proteins.

Correspondence to: Professor Yan Hong, School of Pharmacy, Anhui University of Chinese Medicine, 103 Meishan Road, Hefei, Anhui 230031, P.R. China
E-mail: hyan2003@163.com

Professor Yong-Zhong Wang, Grade 3 Laboratory of Traditional Chinese Medicine Preparation, The First Affiliated Hospital, Anhui University of Chinese Medicine, State Administration of Anhui University of Chinese Medicine, 103 Meishan Road, Hefei, Anhui 230031, P.R. China
E-mail: wyzhmail@163.com

Key words: Rhizoma Paridis saponins, liver fibrosis, angiogenesis, vascular endothelial growth factor, extracellular signal-regulated kinase 1/2

Introduction

Hepatic fibrosis (HF) is a chronic injury to the liver characterized by excess production of extracellular matrix (ECM) proteins. This chronic process undermines the architecture and normal function of the liver, and leads to fibrosis, cirrhosis and eventually hepatocellular carcinoma. Chronic fibrosis, however, is pathological change that may induce organ failure, formation of scar tissue and even result in mortality (1). Previous data has indicated that fibrosis accounts for almost 50% of all-cause mortality in industrialized countries, making this an urgent problem to be solved by clinicians (2).

The pathogenesis of fibrosis is broadly similar, but the regeneration capacity of the liver is remarkable. Therefore, early HF is not readily detected. Angiogenesis is the formation of new blood vessels from pre-existing ones, and it is the stress response of an organism to injury. Hepatic angiogenesis has been observed in different inflammatory, fibrotic and ischemic conditions. Hepatic angiogenesis and overexpression of moieties in hepatic stellate cells (HSCs) are key factors in HF pathogenesis (3). Experimental studies have demonstrated that appropriate anti-angiogenic therapy may lead to significant inhibition of HF progression, decreases in inflammatory infiltrates and α-smooth muscle actin (SMA)-positive myofibroblasts, and a decrease in portal pressure (4,5).

Hepatic angiogenesis is regulated by growth factors expressed by hepatocytes. These growth factors include transforming growth factor (TGF)-β, vascular endothelial growth factor (VEGF), epidermal growth factor, insulin-like growth factor-1, fibroblast growth factor (FGF) and platelet-derived growth factor (PDGF). Levels of these growth factors have been identified to be increased significantly in cases of fibrosis and cirrhosis of the liver.

Among these growth factors, VEGF is the best characterized, due to its mitogenic properties for endothelial cells. Also, its association with angiogenesis and HF has been confirmed. VEGF may induce growth of new blood vessels as a response

to hepatic injury, which is essential for HF (6). In addition, the Ras/Rapidly accelerated fibrosarcoma/mitogen-activated protein kinase kinase/extracellular signal-regulated kinase (ERK) signaling pathway, also known as the ERK pathway, is the most representative of mitogen-activated protein kinase (MAPK) pathways (7), and serves an important part in angiogenesis (8).

HF is the early and only reversible stage of cirrhosis and cancer of the liver (9). Delaying or reversing HF may prevent the development of these pathologies. Therefore, identifying novel drugs that may prevent HF is important.

Rhizoma Paridis grows primarily in Southwest China and, as a traditional Chinese medicine, has been used widely in the treatment of chronic liver disease (10). In certain ethnic groups in China, *Rhizoma Paridis* is used for the treatment of fractures, snake bites and abscesses, due to its heat-clearing and detoxifying properties (11). *Rhizoma Paridis* also exhibits marked anti-tumor activity (12).

Previously, we demonstrated that *Rhizoma Paridis* protects the liver and exhibits anti-HF effects (13). We suggested that the primary active components of *Rhizoma Paridis* that protect against liver injury are *Rhizoma Paridis* saponins (RPS). One of the mechanisms by which RPS is active against HF is the regulation of expression of the RasGAP-activating-like protein 1/ERK1/2 signaling pathway. RPS may inhibit the proliferation and activation of HSCs by inhibiting the ERK pathway and, ultimately, inhibiting or reversing HF (14).

However, the association between VEGF, PDGF and ERKI/2 in HF has not been conclusively demonstrated. The present study aimed to ascertain the effect of RPS on angiogenesis-associated factors including VEGF, PDGF and ERK1/2, and whether RPS exerts anti-HF effects through affecting the VEGF/ERK1/2 pathway, by creating a HF model in rats using carbon tetrachloride (CCl_4).

Materials and methods

RPS preparation. The dried rhizomes of *Rhizoma Paridis* were purchased from the Chinese Herbal Medicine Pharmacy of The First Affiliated Hospital, Anhui University of Chinese Medicine (Hefei, China) following identification by Professor Hua-sheng Pen (Anhui University of Chinese Medicine).

RPS was prepared as described previously (14) and its yield was 1.15%. The content of steroidal saponins in RPS was high when absorbance was measured at 408 nm (53.22 g steroidal saponins/100 g RPS). Ultra-performance liquid chromatography-evaporative light-scattering detection (UPLC-ELSD) was used to determine the contents of the saponins polyphyllin-VII, -VI, -II and -I in RPS in comparison with reference substances as described below, and the contents were identified to be 2.41, 3.15, 2.49 and 9.92%, respectively.

Analyses of RPS by UPLC-ELSD. UPLC-ELSD was performed using an Acquity UPLC H-Class system (Waters Corporation, Milford, MA, USA) consisting of an autosampler and a quaternary pump coupled with an Acquity ELSD detector. An Acquity UPLC BEH C_{18} column (100 mm x 2.1 mm, 1.7 μm, Waters China, Ltd., Shantin, Hong Kong, China) was used for all separations, column temperature was 30˚C and the analysis time was 8 min. UPLC conditions were: Solvent A, acetonitrile; solvent B, water; gradient, 0-2.5 min (40-45% A), 2.5-3.5 min (45-55% A), 3.5-4.5 min (55-60% A), 4.5-6.5 min (65-40% A). The flow rate was 0.45 ml/min, and the injection volume was 2 μl. ELSD conditions were: Gain, 500; nebulizer model, heated; drift tube temperature was 70˚C; gas pressure was 275.8 kPa. The internal standards were saponins polyphyllin-VII (133.6 μg/ml), -VI (84.0 μg/ml), -II (1,1804 μg/ml) and -I (99.6 μg/ml). The UPLC chromatograph of mixed standard compounds and PRS were processed by the Similarity Evaluation Software of Traditional Chinese Medicine Injection (National Pharmacopoeia Commission of China. Edition A, 2004).

Chemicals. CCl_4 was purchased from Sigma-Aldrich; Merck KGaA (Darmstadt, Germany). TRIzol™ was obtained from Invitrogen; Thermo Fisher Scientific, Inc. (Waltham, MA, USA). PCR MasterMix™ was from Thermo Fisher Scientific, Inc. A chemistry analyzer (7600) was purchased from Hitachi, Ltd., (Tokyo, Japan).

Rabbit anti-phosphorylated (p)-ERK1/2 polyclonal antibody was obtained from Cell Signaling Technology, Inc. (cat. no. 4370S, Danvers, MA, USA). VEGF (ab19645), PDGF (aab55160) and α-SMA (ab20979) polyclonal antibodies were purchased from Abcam (Cambridge, UK). ERK1/2 rat anti-human monoclonal antibody (cat. no. 1544S) was purchased from Beijing Biosynthesis Biotechnology Co., Ltd. (Beijing, China). Alanine aminotransferase (ALT; cat. no. c009-2), aspartate aminotransferase (AST; cat. no. c010-2), glutathione (GSH; cat. no. a006-2), malondialdehyde (MDA; cat. no. a003-4) and superoxide dismutase (SOD; cat. no. a001-1-1) kits were obtained from the Nanjing Jiancheng Institute of Biotechnology (Nanjing, China).

Animal experimental model. All experiments were performed in accordance with national legislations and local guidelines. The study protocol was approved by the Committee on the Ethics of Animal Experiments of Anhui University of Chinese Medicine (approval no. 2012AH-036-03).

A total of 40 male Sprague-Dawley rats (180-200 g) were purchased from the Laboratory Animal Center, Medical University of Anhui Province (Hefei, China). Rats were housed in a room with a controlled environment (25˚C and 12 h light-dark cycle) and specific pathogen-free conditions.

After 1 week of acclimation, rats were divided randomly and equally into four groups: Control; model; RPS high dose (RPS-H); and RPS low dose (RPS-L). With the exception of the rats in the control group, rats in each group were injected with 50% CCl_4 dissolved in olive oil (2.0 ml/kg body weight/rat) twice a week for 16 consecutive weeks to induce HF (15,16).

A total of 12 weeks after modeling, the control group was administered the same amount of physiologic (0.9%) saline as gavage; no additional processing was performed in the model group, whereas the RPS-H and RPS-L groups were treated with RPS (300 and 150 mg/10 ml/kg body weight/rat, respectively) once a day as gavage. The optimal dose of PRS was determined in our previous studies, and it was confirmed that the toxicity would not cause harm to the experimental animals at this dose (13,17).

Rats were sacrificed via exsanguination and cervical dislocation at the end of treatment. For 12 h prior to sacrifice,

rats were not fed and anesthetized [2% pentobarbital sodium (40 mg/kg body weight/rat), i.v.], A total of ~10 ml blood was extracted from each rat from the abdominal aorta for measurement of serum biochemical parameters, and liver biopsies from each animal were collected for histology and immunohistochemical (IHC) analyses. The remaining liver samples were snap-frozen to extract total RNA and proteins for molecular analyses.

Liver pathology. Pathological changes in liver tissues were observed by hematoxylin and eosin (H&E; 1%) staining of paraffin sections for 30-60 sec at 25˚C. Tissues were fixed in 4% paraformaldehyde at 55˚C for 1 h. HF extent was determined by Masson trichrome (1%) staining for 5-10 min at 55˚C. Analysis was conducted with an optical light microscope (magnification, x400).

Reverse transcription quantitative polymerase chain reaction (RT-qPCR). Total RNA was extracted from liver samples using TRIzol® (Thermo Fisher Scientific, Inc.) according to the manufacturer's protocol, and stored at -80˚C until use. Then, 3 μg RNA was placed in a 0.2 ml Eppendorf tube for PCR analysis according to the manufacturer's instructions. For RT, an RNA Extraction kit was used, and qPCR was conducted using a Fluorescence Qauntitative PCR kit (both from Sangon Biotech Co., Ltd., Shanghai, China). The thermocycler conditions for RT-qPCR were: Initial denaturation: 95˚C for 5 min, followed by 30 cycles of 95˚C for 10 sec and 60˚C for 30 sec, and final extension was 72˚C for 10 min. The primer for each indicator is summarized in Table I (18).

Western blot analysis. Liver tissues (100 mg) were lysed with 1 ml cell extraction buffer, which was prepared according to methods described previously (14). Lysates were centrifuged at 12,000 x g for 10 min at 4˚C, and the supernatant was collected. Protein samples were separated by SDS-PAGE on 8% gels, transferred to polyvinylidene fluoride (PVDF) membranes and blocked in TBST (TBS buffer with 0.24% Tween-20, pH 7.4, plus 5% skimmed milk powder) for 14-16 h at 4˚C. PVDF membranes were incubated overnight at 4˚C with primary antibodies against VEGF (1:1,000), PDGF (1:1,000), phosphorylated (p)-ERK1/2 (1:2,000), α-SMA (1:1,000) and β-actin (1:800). Following washing 5 times for 10 min each in TBST, bound proteins were detected with a secondary antibody (1:10,000; cat. no. 140829, Tiangen Biochemical Technology (Beijing) Co., Ltd., (Beijing, China) according to manufacturer's instructions. β-actin values were used to normalize expression of VEGF, p-PDGF, p-ERK1/2 and α-SMA. Protein expression was analyzed using ImageJ software (National Institutes of Health, Bethesda, MD, USA).

Measurement of serum biochemical parameters. Blood was collected and centrifuged at 3,000 x g for 10 min at room temperature. The serum was separated and stored at -70˚C. A chemistry analyzer (Bio-Rad Laboratories, Inc., Hercules, CA, USA) was used to determine serum levels of ALT and AST. The thiobarbituric acid reactive substances method (19) was used to measure MDA formation, to determine levels of lipid peroxidation in the liver. Commercial kits were utilized to analyze the activities of SOD and GSH-peroxidase (Px).

Statistical analyses. Data are the mean ± standard deviation. Statistical significance was determined by one-way analysis of variance followed by the Tukey multiple comparisons test. $P<0.05$ was considered to indicate a statistically significant difference. Statistical analyses were performed using SPSS v21.0 (IBM Corp., Armonk, NY, USA).

Results

UPLC-ELSD. Fig. 1 demonstrates that UPLC-ELSD detected 12 peaks within 15 min. Compared with authentic reference substances at individual peak retention times, 4 compounds [polyphyllin-VII (5), polyphyllin-VI (8), polyphyllin-II (9) and polyphyllin-I (11)] were verified in mixed standard compounds; the others were not identified.

Histopathology. The effects of RPS on CCl_4-induced liver injury as evaluated by H&E and Masson's trichrome staining are demonstrated in Fig. 2. There were no significant alterations in the liver tissue of rats in the control group. The hepatic lobular architecture was normal, and little proliferation of connective tissue was noted (Fig. 2A). However, there was massive hepatocellular necrosis in rats of the model group, with alterations in adipose tissue and massive infiltration of lymphocytes causing a severe inflammatory reaction in the portal tract (Fig. 2B). However, the pathological changes induced by CCl_4 treatment were attenuated considerably in RPS-H and RPS-L groups, with decreases in HF, severe steatosis, necrosis and collagen deposition (Fig. 2C and D).

Masson's trichrome staining of liver sections is presented in Fig. 3. The central veins and radiating hepatic cords exhibited an intact lobular architecture in the control group (Fig. 3A). In the model group, hepatic lobules were observed but hepatic cords were irregular. Ballooning degeneration was present, and inflammation was observed in portal areas with proliferation of the small bile ducts. Hyperplasia of collagen fibers was marked and intersected at multiple portal areas. Bridging of collagen fibers connected portal areas with central veins and, as a result, pseudolobuli were formed (Fig. 3B). Compared with the model group, RPS-H and RPS-L groups also exhibited ballooning degeneration, and proliferation of fibrous connective tissue in the portal area. Hepatic lobules were divided by collagen fibers. Pseudolobuli formation was not marked, and hepatic cords were essentially normal (Fig. 3C and D). The RPS-H group was improved compared with the RPS-L group in terms of treatment effect, but the levels of blue staining of the thick fibers in these two groups were markedly decreased compared with the model group following Masson's trichrome staining.

Biochemical parameters. As indicated in Table II, compared with the control group, expression of ALT and AST in the model group was upregulated significantly (4-fold and 2.37-fold higher, respectively, compared with that in the control group). The MDA content was increased compared with that in the control group. These data suggested the successful establishment of a HF model in rats using CCl_4.

The content of SOD and GSH-Px in the model group was decreased compared with that in the control group, with the

Table I. Primer sequences and the length of VEGF, PDGF, ERK1/2 and α-SMA genes.

Gene	Primer sequences (5'-3')	Fragment length, bp	Tm, ˚C
ERK1	F: 5'-CCATCCCAAGAGGACCTAAA-3'	273	55
	R: 5'-ATCATCCAGCTCCATGTCAA-3'		
ERK2	F: 5'-CGCGCTACACTAATCTCTCG-3'	470	58
	R: 5'-ATCATGGTCTGGATCTGCAA-3'		
VEGF	F: 5'-GTCTACCAGCGCAGCTATTG-3'	491	97
	R: 5'-AGTCGAGTCGGAAAGCTCAT-3'		
PDGF	F: 5'-CACAGGACGGCTTGAAGATA-3'	355	101
	R: 5'-ACACCTCTGTACGCGTCTTG-3'		
GAPDH	F: 5'-CAAGGTCATCCATGACAACTTTG-3'	496	55
	R: 5'-GTCCACCACCCTGTTGCTGTAG-3'		

ERK1/2, extracellular signal-regulated kinase 1/2; VEGF, vascular endothelial growth factor; PDGF, platelet-derived growth factor; F, forward; R, reverse.

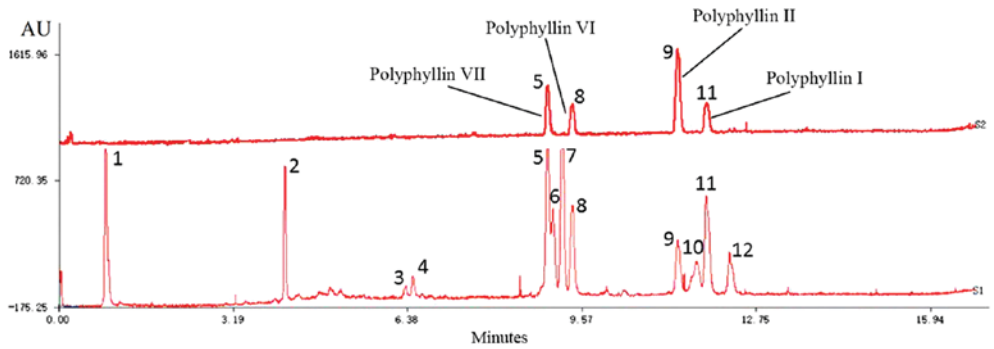

Figure 1. Ultra-performance liquid chromatography-evaporative light-scattering detection chromatograms of (S1) mixed standard compounds and (S2) *Rhizoma Paridis* saponins sample.

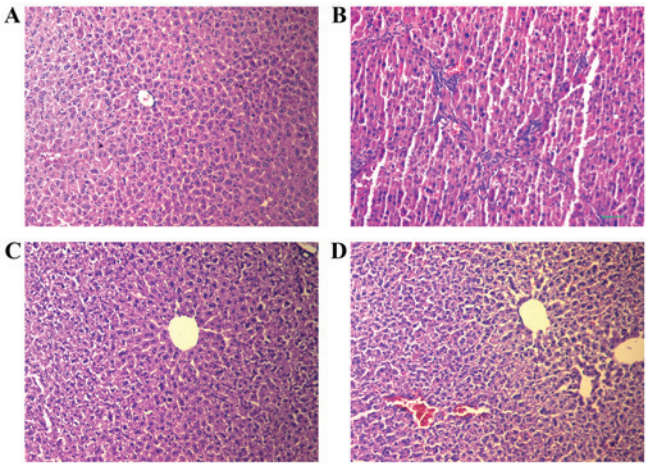

Figure 2. Effects of RPS against CCl_4-induced hepatic fibrosis in rats based on hematoxylin and eosin staining. (A) Control group. (B) Model group. (C) RPS-High dose (300 mg/kg). (D) RPS-Low dose (150 mg/kg). Images are at magnification, x400. Scale bar=50 μm. RPS, *Rhizoma Paridis* saponins.

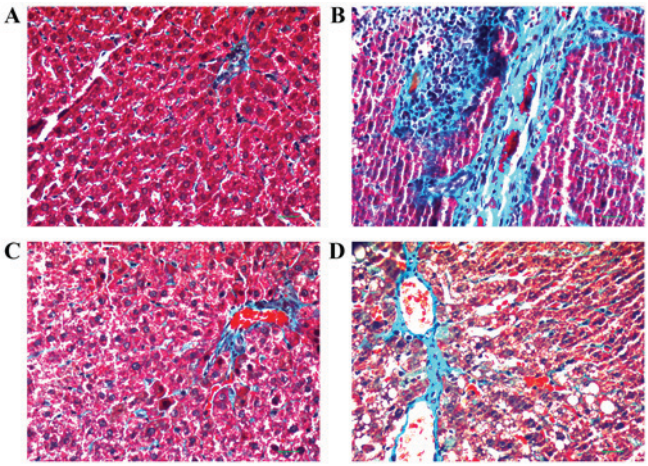

Figure 3. Effects of RPS against CCl_4-induced hepatic fibrosis in rats based on Masson trichrome staining. (A) Control group. (B) Model group. (C) RPS-High dose (300 mg/kg). (D) RPS-Low dose (150 mg/kg). Images are at magnification, x400. RPS, *Rhizoma Paridis* saponins.

GSH-Px content exhibiting a significant decrease. However, a significant decrease in expression of ALT and AST in the RPS-H and RPS-L groups was observed compared with the model group. The MDA content also decreased in RPS-H and RPS-L groups compared with the model group. Expression of SOD and GSH-Px in the RPS-H and RPS-L groups exhibited marked upregulation compared with the model group and was close to that observed in the control group. These results

Table II. Alterations in serum biochemical parameters and activity of antioxidant enzymes.

Groups	n	ALT (U/l)	AST (U/l)	MDA (nmol/mg protein)	SOD (U/mg protein)	GSH (U/mg protein)
Control	10	20.64±4.38	47.30±6.41	0.82±0.09	98.45±17.50	273.26±44.37
Model	10	80.91±18.93[a]	112.50±19.23[a]	1.20±0.18[a]	70.34±14.74[a]	165.65±49.21[a]
RPS H	10	51.14±14.70[b]	80.80±22.60[b]	0.90±0.12[b]	84.70±15.31[c]	244.21±55.62[b]
RPS L	10	60.52±10.29[b]	92.50±19.76[c]	1.03±0.15[c]	79.10±12.90	220.91±66.08[c]

Values are presented as means ± standard deviation. Statistical analysis was performed by one-way analysis of variance. [a]P<0.01 vs. the Control group; [b]P<0.01 and [c]P<0.05 vs. Model group. RPS, *Rhizoma Paridis* saponins; H, high dose; L, low dose; ALT, Alanine aminotransferase; AST, aspartate aminotransferase; MDA, malondialdehyde; SOD, superoxide dismutase; GSH, glutathione.

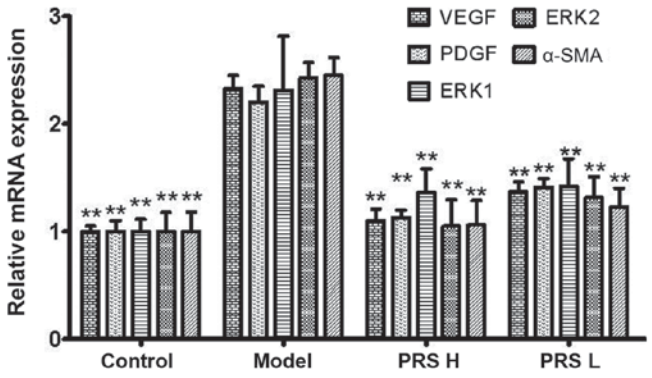

Figure 4. mRNA expression for VEGF, PDGF, ERK1/2 and α-SMA using reverse transcription quantitative polymerase chain reaction. **P<0.01 vs. the model group. VEGF, vascular endothelial growth factor; PDGF, platelet-derived growth factor; ERK1/2, extracellular signal-regulated kinase 1/2; α-SMA, α smooth muscle actin; RPS, *Rhizoma Paridis* saponins; H, high dose; L, low dose.

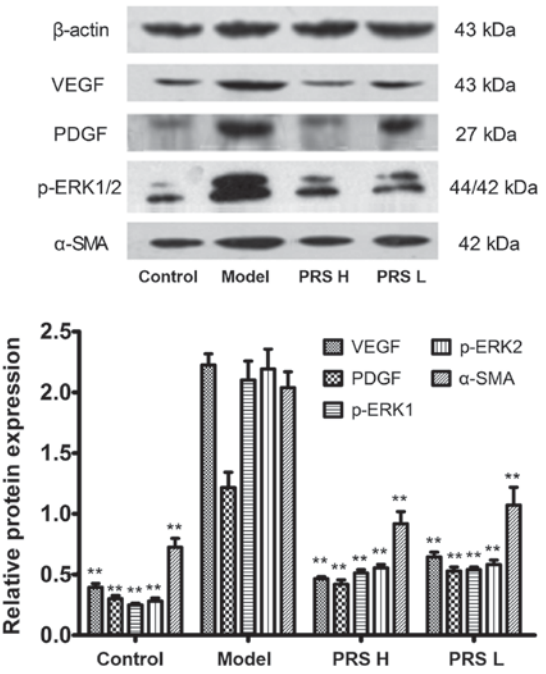

Figure 5. Western blot analysis of protein expression of VEGF, PDGF, ERK1/2 and α-SMA. **P<0.01 vs. the model group. VEGF, vascular endothelial growth factor; PDGF, platelet-derived growth factor; ERK1/2, extracellular signal-regulated kinase 1/2; α-SMA, α smooth muscle actin; RPS, *Rhizoma Paridis* saponins; H, high dose; L, low dose.

demonstrated the robust anti-HF effects of RPS: It was able to increase the activity of SOD and GSH-Px and inhibit lipid peroxidation in liver tissue simultaneously. Therefore, RPS may protect the liver from oxygen free radicals and peroxides.

mRNA expression of VEGF, PDGF, ERK1/2 and α-SMA. mRNA expression of VEGF, PDGF, ERK1/2 and α-SMA in the model group was 2.33-, 2.20-, 2.31-, 2.43- and 2.45-fold increased, respectively, compared with that in the control group (Fig. 4). Compared with the model group, relative mRNA expression of VEGF, PDGF, ERK1/2 and α-SMA in the RPS groups was decreased significantly (P<0.01). The decrease in the RPS-H group was even more significant compared with that observed in the RPS-L group. These results suggested that RPS treatment of HF in rats may be through downregulation of expression of angiogenic growth factors in liver tissue, thereby improving liver microcirculation.

Protein expression of VEGF, PDGF, p-ERK1/2 and α-SMA. Protein expression of VEGF, PDGF, p-ERK1/2 and α-SMA in the model group was markedly increased compared with that in the control group (Fig. 5). Following RPS treatment, the protein expression levels of VEGF, PDGF, p-ERK1/2 and α-SMA were decreased significantly (P<0.01) compared with the model group. The results suggested that the decrease of VEGF, PDGF, p-ERK1/2 and α-SMA expression may be one of the mechanisms by which PRS improves liver fibrosis.

Discussion

HF is the result of abnormal proliferation of connective tissue, and proliferation of connective tissue is a wound-healing response to various types of chronic injury to the liver, for example viral infection and exposure to chemicals (20). At the molecular level, HF pathogenesis is closely associated with HSCs. The latter may undergo trans-differentiation into fibrogenic, proliferative and contractile myofibroblasts (21). Apoptosis and soluble growth factors may lead to HSC stimulation. Specific lymphocyte subsets may induce HF. A signaling cascade and transcription are the basis of fibrogenic effects in HSCs, and each factor in the cascade may be a target for anti-HF therapy (22). Several vitamins are stored in HSCs.

If the liver is damaged, release of vitamin A is decreased in HSCs, but increased expression of α-SMA promotes HF (23). VEGF, PDGF, ERK and TGF-β may also activate HSCs.

Abnormal expression of VEGF occurs under pathological conditions. In ischemic disease, hypoxia may stimulate VEGF expression. The resulting marked induction of mitosis of endothelial cells promotes formation of new blood vessels and improves the blood supply to tissue. VEGF is a key factor for ocular neovascularization, and promotes the formation and development of new blood vessels directly; its expression is closely associated with disease severity (24).

ERK1/2 belongs to the family of MAPKs which are involved in the regulation of the proliferation, differentiation, growth and apoptosis of cells. The term ERK1/2 refers to two closely associated kinase isoforms (25). ERK enters the nucleus subsequent to activation, causing changes in the expression of genes for the substrate, and affecting the growth and proliferation of cells. The present study identified that ERK was phosphorylated in the MAPK and VEGF pathways. It has also been identified that upregulation of p-ERK1/2 was induced by CCl_4 in previous studies (26,27). Injury primarily affects the post-translational modification of ERK1/2. The effects of injury on ERK1/2 was demonstrated by drug treatment, indicating the reversal of liver fibrosis; that is, whether the regulation of p-ERK exists. Therefore, ERK expression is closely associated with HF. In addition, a previous study (14), ERK1/2 protein has been determined by immunohistochemistry. Therefore, the present study selected to detect p-ERK1/2.

The VEGF/ERK1/2 signaling pathway has been demonstrated to serve a key role in the proliferation of endothelial cells (28). In bovine retinal microvascular endothelial cells *in vitro*, VEGF stimulated ERK1/2 phosphorylation in a dose-dependent manner to promote the formation and proliferation of endothelial cells (29). VEGF and other growth factors affect cellular functions through the ERK pathway. They promote the transcription and expression of selected genes, and thereby initiate the proliferation and differentiation of cells. This signaling pathway has an important role in the growth, development and proliferation of cells (30). In the present study, expression levels of VEGF and p-ERK1/2 in the model group were high; in the RPS treatment groups, expression of VEGF and p-ERK1/2 was decreased accordingly. Therefore, we hypothesized that the VEGF/ERK1/2 pathway has a prominent role in HF.

Traditionally, PDGF has been considered to be an important fibrogenic and proliferative stimulus to HSCs (31). The PDGF family of ligands and receptors regulate multiple processes. They are also involved in several pathologic events, including cancer and fibrotic diseases (32). During the pathogenesis of fibrotic diseases, PDGF serves a major role in stimulating the replication, survival and migration of myofibroblasts, and several pro-inflammatory cytokines mediate their mitogenic effects via autocrine release of PDGF. PDGF is a potent mitogen that may aid fibroblast proliferation and secrete fibronectin in liver fibroblasts (33,34). Large amounts of PDGF stimulate the ERK1/2 pathway and promote HSC proliferation.

An additional important fibrogenic mediator, TGF-β, induces secretion of VEGF, FGF and endothelin-1, thereby resulting in HF. VEGF and FGF-2 induce hepatic vascular proliferation during HF, and VEGF has an important role in the angiogenesis of HF. VEGF may also activate HSCs via autocrine or paracrine pathways (35,36). VEGF induces expression of different proteases by endothelial cells, and stimulation of endothelial cells and pro-coagulant activity in monocytes may induce microvascular remodeling in the liver indirectly; the final stage involves HF development.

α-SMA expression is upregulated together with an increased ECM during HSC activation in HF. α-SMA is an important symbol of HSC activation (37,38). Therefore, understanding which growth factors are expressed aberrantly in the signaling cascade and transcription for HSCs is paramount for developing treatment strategies for HF.

Previously, we demonstrated that RPS exhibits hepatoprotective and antifibrotic effects *in vivo* against HF induced by CCl_4 (14). The anti-HF action of RPS may involve the RAS/ERK1/2 signaling pathway. In the present study, the expression levels of VEGF, PDGF, ERK1/2, and α-SMA were measured to explore the mechanism of action of RPS against HF.

It was identified that CCl_4 intoxication damaged liver function, caused hepatocyte necrosis, and upregulated the expression levels of the mRNA and phosphorylated proteins of VEGF, PDGF, ERK1/2 and α-SMA. By contrast, following oral administration of RPS the severity of HF was relieved significantly, according to histopathology. Furthermore, the expression levels of the mRNA and phosphorylated protein of VEGF, PDGF, ERK1/2 and α-SMA were decreased. The results suggested that RPS exhibited anti-HF effects in rat livers *in vivo*. Therefore, downregulation of the VEGF/ERK pathway and improvement of angiogenesis may be associated with the anti-HF action of RPS.

Acknowledgements

The authors appreciate the technical support provided by Shanghai Aoji Biotechnology Co., Ltd. (Shanghai, China).

Funding

The present study was supported by a grant from the Clinical Research Fund of Anhui University of Chinese Medicine (grant no. 2012zr010).

Availability of data and materials

All data generated or analyzed during this study are included in this published article.

Authors' contributions

YHa conceived and designed the study. LP designed the schema of the VEGF/ERK1/2 signaling and drafted the manuscript. SR, YS and FFS performed the experiments. YZW and YHo analyzed the data. All authors read and approved the final manuscript.

Ethics approval and consent to participate

All experiments were performed in accordance with national legislations and local guidelines. The study protocol was approved by the Committee on the Ethics of Animal

Experiments of Anhui University of Chinese Medicine (approval no. 2012AH-036-03).

Patient consent for publication

Not applicable.

Competing interests

The authors declare that they have no competing interests.

References

1. Zoheir KMA, Amara AA, Ahmad SF, Mohammad MA, Ashour AE, Harisa G and Abd-Allah AR: Study of the therapeutic effects of Lactobacillus and α-lipoic acid against dimethylnitrosamine-induced liver fibrosis in rats. J Genet Eng Biotechnol 12: 135-142, 2014.
2. Friedman SL: Hepatic fibrosis: Emerging therapies. Dig Dis 33: 504-507, 2015.
3. Elzamly S, Agina HA, Elbalshy AE, Abuhashim M, Saad E and Abd Elmageed ZY: Integration of VEGF and α-SMA expression improves the prediction accuracy of fibrosis in chronic hepatitis C liver biopsy. Appl Immunohistochem Mol Morphol 25: 261-270, 2017.
4. Fernández M, Semela D, Bruix J, Colle I, Pinzani M and Bosch J: Angiogenesis in liver disease. J Hepatol 50: 604-620, 2009.
5. Valfrè di Bonzo L, Novo E, Cannito S, Busletta C, Paternostro C, Povero D and Parola M: Angiogenesis and liver fibrogenesis. Histol Histopathol 24: 1323-1341, 2009.
6. Giatromanolaki A, Kotsiou S, Koukourakis MI and Sivridis E: Angiogenic factor expression in hepatic cirrhosis. Mediators Inflamm 2007: 67187, 2007.
7. Dhillon AS, Hagan S, Rath O and Kolch W: MAP kinase signalling pathways in cancer. Oncogene 26: 3279-3290, 2007.
8. Yang F, Li J, Zhu J, Wang D, Chen S and Bai X: Hydroxysafflor yellow A inhibits angiogenesis of hepatocellular carcinoma via blocking ERK/MAPK and NF-κB signaling pathway in H22 tumor-bearing mice. Eur J Pharmacol 754: 105-114, 2015.
9. Li DS: 45 cases clinical observation of matrine in treatment of liver fibrosis of patients with chronic hepatitis. China Ming Kang Med 23: 2701-2703, 2011 (In Chinese).
10. Man S, Fan W, Liu Z, Gao W, Li Y, Zhang L and Liu C: Antitumor pathway of *Rhizoma Paridis* saponins based on the metabolic regulatory network alterations in H22 hepatocarcinoma mice. Steroids 84: 17-21, 2014.
11. Man S, Gao W, Zhang Y, Jin X, Ma C, Huang X and Li Q: Characterization of steroidal saponins in saponin extract from Paris polyphylla by liquid chromatography tandem multi-stage mass spectrometry. Anal Bioanal Chem 395: 495-505, 2009.
12. Man S, Gao W, Zhang Y, Yan L, Ma C, Liu C and Huang L: Antitumor and antimetastatic activities of *Rhizoma Paridis* saponins. Steroids 74: 1051-1056, 2009.
13. Hong Y, Han Y, Luo H, Gui J, Zhang K and Jiang H: Effect of Chonglou saponin on markers of liver fibrosis of hepatic fibrosis rats and correlation analysis. J Shanxi Coll Trad Chin Med 15: 20-22+67, 2014 (In Chinese).
14. Hong Y, Han YQ, Wang YZ, Gao JR, Li YX, Liu Q and Xia LZ: *Paridis Rhizoma* sapoinins attenuates liver fibrosis in rats by regulating the expression of RASAL1/ERK1/2 signal pathway. J Ethnopharmacol 192: 114-122, 2016.
15. Sun H, Che QM, Zhao X and Pu XP: Antifibrotic effects of chronic baicalein administration in a CCl4 liver fibrosis model in rats. Eur J Pharmacol 631: 53-60, 2010.
16. Vatakuti S, Schoonen WG, Elferink ML, Groothuis GM and Olinga P: Acute toxicity of CCl4 but not of paracetamol induces a transcriptomic signature of fibrosis in precision-cut liver slices. Toxicol In Vitro 29: 1012-1020, 2015.
17. Liu Z, Gao W, Man S, Wang J, Li N, Yin S, Wu S and Liu C: Pharmacological evaluation of sedative-hypnotic activity and gastro-intestinal toxicity of *Rhizoma Paridis* saponins. J Ethnopharmacol 144: 67-72, 2012.
18. Livak KJ and Schmittgen TD: Analysis of relative gene expression data using real-time quantitative PCR and the 2(-Delta Delta C(T)) method. Methods 25: 402-408, 2001.
19. Matsushita T, Inoue SI and Tanaka R: An assay method for determining the total lipid content of fish meat using a 2-thiobarbituric acid reaction. J Am Oil Chem Soc 87: 963-972, 2010.
20. Choi JH, Sun WJ, Kim HG, Khanal T, Hwang YP, Lee KJ, Choi CY, Chung YC, Lee YC and Jeong HG: Platycodi Radix attenuates dimethylnitrosamine-induced liver fibrosis in rats by inducing Nrf2-mediated antioxidant enzymes. Food Chem Toxicol 56: 231-239, 2013.
21. Feng Y, Cheung KF, Wang N, Liu P, Nagamatsu T and Yao T: Chinese medicines as a resource for liver fibrosis treatment. Chin Med 4: 16, 2009.
22. Wells RG: The role of matrix stiffness in hepatic stellate cell activation and liver fibrosis. J Clin Gastroenterol 39 (Suppl 2): S158-S161, 2005.
23. D'Argenio G, Mazzone G, Ribecco MT, Lembo V, Vitaglione P, Guarino M, Morisco F, Napolitano M, Fogliano V and Caporaso N: Garlic extract attenuating rat liver fibrosis by inhibiting TGF-β1. Clin Nutr 32: 252-258, 2013.
24. Ding Q, Tian XG, Li Y, Wang QZ and Zhang CQ: Carvedilol may attenuate liver cirrhosis by inhibiting angiogenesis through the VEGF-Src-ERK signaling pathway. World J Gastroenterol 21: 9566-9576, 2015.
25. Keyse SM: Protein phosphatases and the regulation of mitogen-activated protein kinase signalling. Curr Opin Cell Biol 12: 186-192, 2000.
26. Sung YC, Liu YC, Chao PH, Chang CC, Jin PR, Lin TT, Lin JA, Cheng HT, Wang J, Lai CP, *et al*: Combined delivery of sorafenib and a MEK inhibitor using CXCR4-targeted nanoparticles reduces hepatic fibrosis and prevents tumor development. Theranostics 8: 894-905, 2018.
27. Gao Q, Gu Y, Jiang Y, Fan L, Wei Z, Jin H, Yang X, Wang L, Li X, Tai S, *et al*: Long non-coding RNA Gm2199 rescues liver injury and promotes hepatocyte proliferation through the upregulation of ERK1/2. Cell Death Dis 9: 602, 2018.
28. Yuan LH, Chen XL, Di Y and Liu ML: CCR7/p-ERK1/2/VEGF signaling promotes retinal neovascularization in a mouse model of oxygen-induced retinopathy. Int J Ophthalmol 10: 862-869, 2017.
29. Bullard LE, Qi X and Penn JS: Role for extracellular signal-responsive kinase-1 and -2 in retinal angiogenesis. Invest Ophthalmol Vis Sci 44: 1722-1731, 2003.
30. Johnson GL and Lapadat R: Mitogen-activated protein kinase pathways mediated by ERK, JNK, and p38 protein kinases. Science 298: 1911-1912, 2002.
31. Gressner AM: Transdifferentiation of hepatic stellate cells (Ito cells) to myofibroblasts: A key event in hepatic fibrogenesis. Kidney Int Suppl 54: S39-S45, 1996.
32. Lenz B, Klafki HW, Hillemacher T, Frieling H, Clepce M, Gossler A, Thuerauf N, Winterer G, Kornhuber J and Bleich S: ERK1/2 protein and mRNA levels in human blood are linked to smoking behavior. Addict Biol 17: 1026-1035, 2012.
33. Bonner JC: Regulation of PDGF and its receptors in fibrotic diseases. Cytokine Growth Factor Rev 15: 255-273, 2004.
34. Gallini R: A PDGFRalpha perspective on PDGF signalling in developmental and pathological processes. Geobiology 7: 360-372, 2014.
35. Chaudhary NI, Roth GJ, Hilberg F, Müller-Quernheim J, Prasse A, Zissel G, Schnapp A and Park JE: Inhibition of PDGF, VEGF and FGF signalling attenuates fibrosis. Eur Respir J 29: 976-985, 2007.
36. Rosmorduc O, Wendum D, Corpechot C, Galy B, Sebbagh N, Raleigh J, Housset C and Poupon R: Hepatocellular hypoxia-induced vascular endothelial growth factor expression and angiogenesis in experimental biliary cirrhosis. Am J Pathol 155: 1065-1073, 1999.
37. Corpechot C, Barbu V, Wendum D, Kinnman N, Rey C, Poupon R, Housset C and Rosmorduc O: Hypoxia-induced VEGF and collagen I expressions are associated with angiogenesis and fibrogenesis in experimental cirrhosis. Hepatology 35: 1010-1021, 2002.
38. Nielsen MJ, Nielsen SH, Hansen NUB, Kristensen JH, Karsdal MA and Leeming DJ: P0525: N-Acetylated alpha smooth muscle actin levels are increased in hepatic fibrosis but decreased in hepatocellular carcinoma. J Hepatology 62: S512, 2015.